Available online at www.sciencedirect.com
ScienceDirect
Ceramics International 35 (2009) 1187–1193
CERAMICS INTERNATIONAL
www.elsevier.com/locate/ceramint

Microstructure and mechanical properties of TiC–TiN–Zr–WC–Ni–Co cermets

Xiaobo Zhang, Ning Liu *, Chunlan Rong, Jun Zhou

School of Materials Science and Engineering, Hefei University of Technology, 193 Tunxi Road, Hefei 230009, PR China

Received 7 December 2007; received in revised form 8 April 2008; accepted 1 June 2008
Available online 16 July 2008

Abstract

Cermet cutting tools are widely used for semi-finishing and finishing work on steel and cast iron. However, their brittleness is still an unavoidable limitation for their utilizations. Zirconium was added to improve the fracture toughness of Ti(C, N) based cermets. The microstructure and the fracture surfaces of cermets were studied by using scanning electron microscopy (SEM) and energy dispersive spectroscopy (EDS). The experimental results reveal that Zr dissolved and formed solid solutions during the sintering process. The amount of grains with typical core/rim structure decreases and that of coreless grains increases with increasing Zr addition. Moreover, the fracture toughness is improved clearly due to the increased amount of the coreless grains, the spinodal decomposition in cermets, as well as the crack deflection and crack branching mechanisms. Additionally, hardness and relative density were also measured, respectively.

Keywords: B. Grain size; C. Mechanical properties; Microstructure; Zirconium

1. Introduction

Titanium carbonitride based cermets have been successfully introduced in the metal cutting industry. They own several better properties compared with conventional WC–Co cemented carbides and even with coated cemented carbides. Several basic features are responsible for the superior cutting performance of cermets: high cutting speed at moderate chip cross-sections, high surface quality of the machined work piece, high wear resistance, high performance reliability, high edge strength and edge sharpness which are particularly important for meeting demands of near net shape technology and the machining of thin-walled items [1]. The physical and mechanical properties of cermets can be adjusted within certain limits to meet the requirements of the cutting task. Hardness increases with increasing TiC or TiN content, whereas, additions of (Ta, Nb)C appear to improve the cutting performance in interrupted cuts or in milling applications. With increased additions of Mo_2C or WC, full densification during sintering becomes less of a problem [2–6]. However, because of relatively low fracture toughness and low thermal shock resistance, Ti(C, N) based cermets are still limited for wider utilization.

Fracture toughness is defined by the propagation of crack through the phase of the composites. In fact, the toughness of materials depends on the flow stress of the binder, and the contribution of the binder to the fracture toughness is much greater than that of the ceramic phase [7], hence better toughness would be obtained with more binder, but this is at the cost of losing hardness [8]. Cermets fabricated by ultra-fine or nano initial powders can obtain excellent strength and hardness according to the Hall–Petch formula, but with losing a little fracture toughness [9]. Consequently, the improvement of the fracture toughness of Ti(C, N) based cermets is of great interest and importance in the modern machining process.

Ti(C, N) based cermets consist of two phases: ceramic phase (titanium carbonitride) and metal phase (nickel or cobalt or a mixture of them) [10,11]. Microstructure observation shows that a typical carbonitride grain often exhibits a stable core/rim structure: Ti(C, N) cores surrounded by (Ti, W, Mo, Nb, Ta,...) (C, N) complex carbonitride rims. The undissolved Ti(C, N) cores are responsible for the high hardness and the excellent wear resistance, while the cubic carbides (Ti, W, Mo, Nb, Ta,...) (C, N) solid solution rims and the metal binder phase

* Corresponding author. Tel.: +86 551 2909865; fax: +86 551 2905383.
E-mail address: ningliu@mail.hf.ah.cn (N. Liu).

0272-8842/$34.00 © 2008 Published by Elsevier Ltd and Techna Group S.r.l.
doi:10.1016/j.ceramint.2008.06.005

contribute to toughness, ductility, integrity and thermal shock resistance [7,12]. The rim phases, which are formed around the cubic TiC or Ti(C, N) cores via dissolution–reprecipitation process during liquid-phase sintering, are composed of a mixture of Ti(C, N) and secondary carbides, such as WC and Mo_2C [13]. Furthermore, the rim phase sometimes exhibits two types: inner rim and outer rim, the inner rim should be developed by chemical reaction of Ti(C, N) and Mo_2C before the formation of the liquid phase, and the outer rim should be formed by precipitation of the carbides dissolved in the liquid metal [14]. The rim phase in Ti(C, N) based cermets with a typical core/rim structure is responsible for the improved properties. Cermets only consisting of (Ti, M)C or (Ti, M)(C, N)-type rim phase microstructure have been pursued since the 1980s. However, few of them have been obtained by conventional powder metallurgy technique. Kim et al. [15] and Park and Kang [16] synthesized cermets without core/rim structure (coreless grains) by using (Ti, Mo)C–Ni, nano-crystalline (Ti, W)C–Ni and (Ti, W) (C, N)–Ni powders, and results showed that the toughness was significantly improved. Furthermore, several fracture mechanisms can be introduced to toughen ceramics, such as martensitic transformation of zirconia from the tetragonal to monoclinic phase, micro-crack formation, crack deflection, crack branching, crack bridging and fiber toughening [17,18].

Spinodal decomposition is a mechanism for phase separation that leads to a characteristic modulated structure which can be exploited to control microstructure at the nanometer scale. Numerous metal oxide and non-oxide systems, such as TiO_2–SnO_2 [19], Ti–Cr [20], Fe–Cr [21] and Cu–Ni–Sn [22], are known to decompose through spinodal mechanisms. Moreover, Ti–Mo–C–N system undergoes a spinodal phase separation [23].

Zirconium has been widely studied in alloys, but it has not been added into Ti(C, N) based cermets yet. The aim of the study is to investigate the effect of zirconium on the microstructure and mechanical properties, especially fracture toughness of cermets in order to supply the basis for application.

2. Experimental

TiC–TiN–WC–Zr–Ni–Co series cermets were fabricated. The composition is listed in Table 1. Commercially available TiC (2.56 μm), TiN (3.50 μm), WC (3.52 μm), Co (2.46 μm), Ni (2.95 μm), Zr (7.40 μm), and C (3.25 μm) powders were used as initial materials. The mean particle sizes were measured by a Malven Mastersizer-2000 laser particle size analyzer. Four compositions were designed as listed in Table 1. Powder mixtures were milled with WC–Co balls by a planetary ball in an ethanol bath for 24 h and then dried. Green compacts were prepared by pressing at the uniaxial pressure of 170 MPa, dewaxed at 800 °C at heating rate of 0.5 °C/min, finally vacuum sintered (0.1 Pa) at 1430 °C for 1 h.

Table 1
Composition of tested cermets (wt%)

Cermets	TiC	TiN	Zr	WC	Co	Ni	C
A	58.5	10	0	15	7.5	7.5	1.5
B	48.5	10	10	15	7.5	7.5	1.5
C	43.5	10	15	15	7.5	7.5	1.5
D	38.5	10	20	15	7.5	7.5	1.5

The microstructure of polished specimens was observed by a scanning electron microscope (SEM) in back-scattered electron (BSE) mode. The fracture surface morphology was observed by SEM in secondary electron (SE) mode and the composition analysis was conducted by an energy dispersive spectroscope (EDS). The phase identification of each system was carried out by an X-ray diffractometer. Rockwell hardness was measured on a common Rockwell hardometer under a load of 60 kg. Fracture toughness was examined by indentation method under indentation load of 30 kg, using the expression derived by Shetty et al. [24]:

$$K_{IC} = 0.0889\left(\frac{H_V P}{4l}\right)^{1/2} \quad (1)$$

where H_V is the Vicker's hardness, P is the indentation load and l is the crack length.

The relative density of each cermet is the ratio between the actual density and the theoretical one. The theoretical densities of cermets, $d_{theoretical}$, were calculated by the formula:

$$d_{theoretical} = \frac{100\%}{(a\%/d_a) + (b\%/d_b) + \cdots} \quad (2)$$

where $a\%$, $b\%$ are the ratios of the starting compositions (wt%), and d_a, d_b are the theoretical densities of the initial compositions.

The actual densities of cermets, d_{actual}, were measured by using Archimedes method with distilled water and calculated by the formula:

$$d_{actual} = \frac{G_1}{G_1 + G_2 - G_3} d_{H_2O} \quad (3)$$

where G_1 is the weight of the sample, G_2 is the weight of the thin copper line, G_3 is the weight of sample and line in distilled water and $d_{H_2O} = 1.0 g/cm^3$ is the density of the distilled water.

3. Results and discussion

3.1. Phase analysis of cermets

Fig. 1 shows the X-ray diffraction profiles of cermets. The analytical results show that (Ti, W)(C, N) phases exist in cermets after sintering. The peaks of the solid solution (Ti, Zr, W)(C, N) cannot be identified because it is difficult to distinguish between the peaks of (Ti, W)(C, N) and (Ti, Zr, W)(C, N) phases. Zr was dissolved in the binder and reprecipitated as (Ti, Zr, W)(C, N) solid solution, which has the same crystal structure and similar lattice parameters as (Ti, W)(C, N). Therefore, the peaks of (Ti, Zr, W)(C, N) solid solution and (Ti, W)(C, N) superimpose together. Moreover, other peaks are detected when Zr element is added, and the

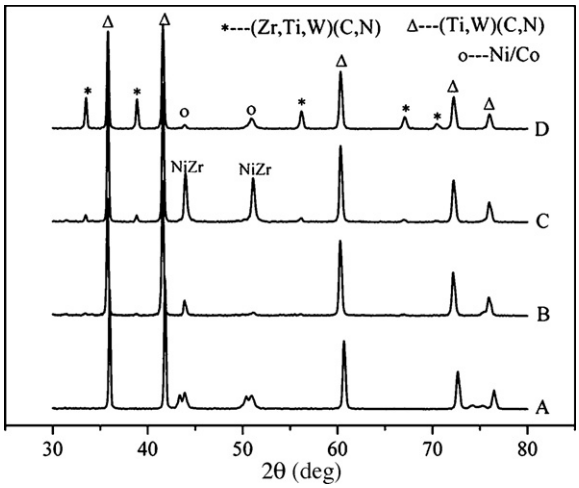

Fig. 1. X-ray diffraction profiles of cermets. (A) 0% Zr, (B) 10% Zr, (C) 15% Zr, (D) 20% Zr.

intensity of these peaks gets stronger with increasing Zr. These peaks are very close to those of ZrC. We suppose that the amount of Zr-rich (Zr, Ti, W)(C, N) particles increases with the increase of Zr content. Meanwhile, more sites for the precipitation in the system are provided so that more (Zr, Ti, W)(C, N) solid solution grains are formed. Consequently, these peaks should belong to (Zr, Ti, W)(C, N) solid solutions.

Diffraction peaks belonging to both Ni and Co are found in the cermets without Zr (Fig. 1). Ni and Co peaks get together with increasing Zr content because Zr contributes to the formation of solid solution of Co and Ni. It is noted that the intensity of Co and Ni in cermet C is much stronger than those of any other samples. The total content of Co and Ni is a constant (15 wt%), so there should be another phase present which has the same crystal structure and similar lattice parameters as Co and Ni. It is known that Zr can form carbonitrides easily. So we guess that when the content of Zr is low, it is dissolved in the binder, and then (Ti, Zr, W)(C, N) solid solution is formed during the liquid sintering by dissolution–reprecipitation mechanism. But there must be some extra Zr in the binder when its content increases, so extra Zr is likely to accelerate the formation of metallic compound Ni(Co)Zr in the binder, and the lattice parameters of Ni(Co)Zr are very close to those of Co and Ni.

However, the intensity of the binder lowers in cermet D while the intensity of the (Zr, Ti, W)(C, N) solid solution enhances evidently. As mentioned above, more Zr-rich particles served as the sites for precipitation with increasing Zr content. Therefore, there might be no Ni(Co)Zr metallic compound in cermet D.

3.2. Effect of Zr on the microstructure of cermets

Typical back-scattered SEM micrographs of various cermets are shown in Fig. 2. It is visible that the typical black core/grey rim ceramic grains embed into the metallic binder phase (Fig. 2a). However, the microstructure of cermets is different from cermet A with increasing Zr content (from Fig. 2b–d): white core/grey rim ceramic grains appear, more grey and bright coreless ceramic grains exist, the microstructure gets

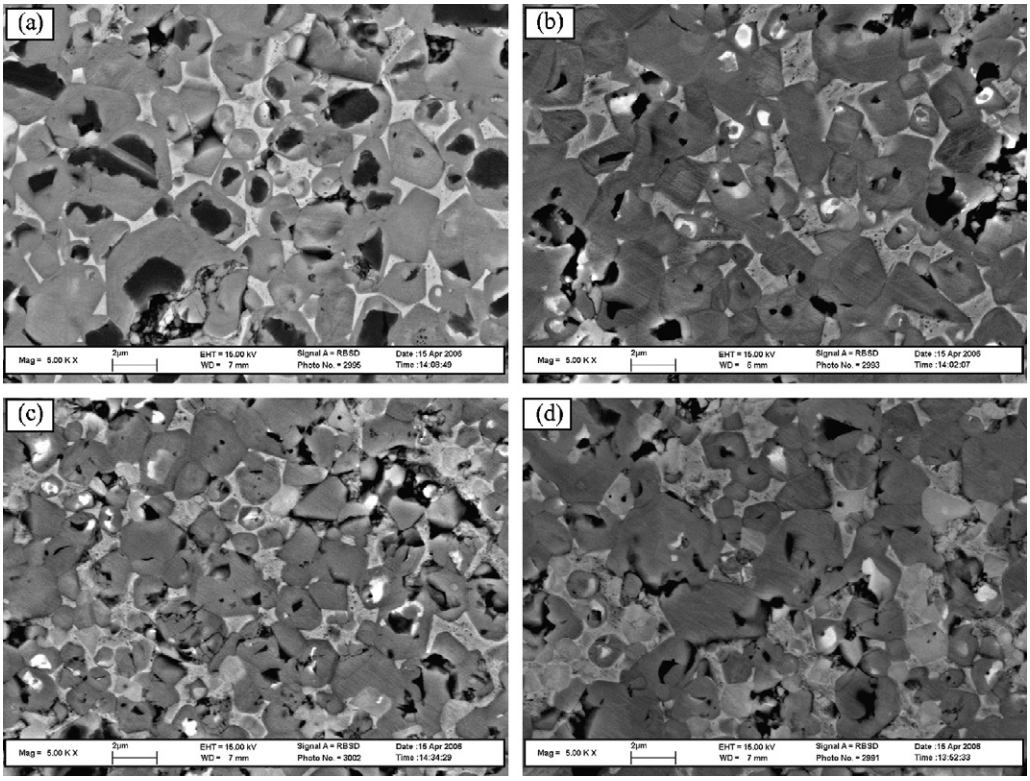

Fig. 2. SEM (BSE) photographs of microstructure with various zirconium contents. (a) 0% Zr, (b) 10% Zr, (c) 15% Zr, (d) 20% Zr.

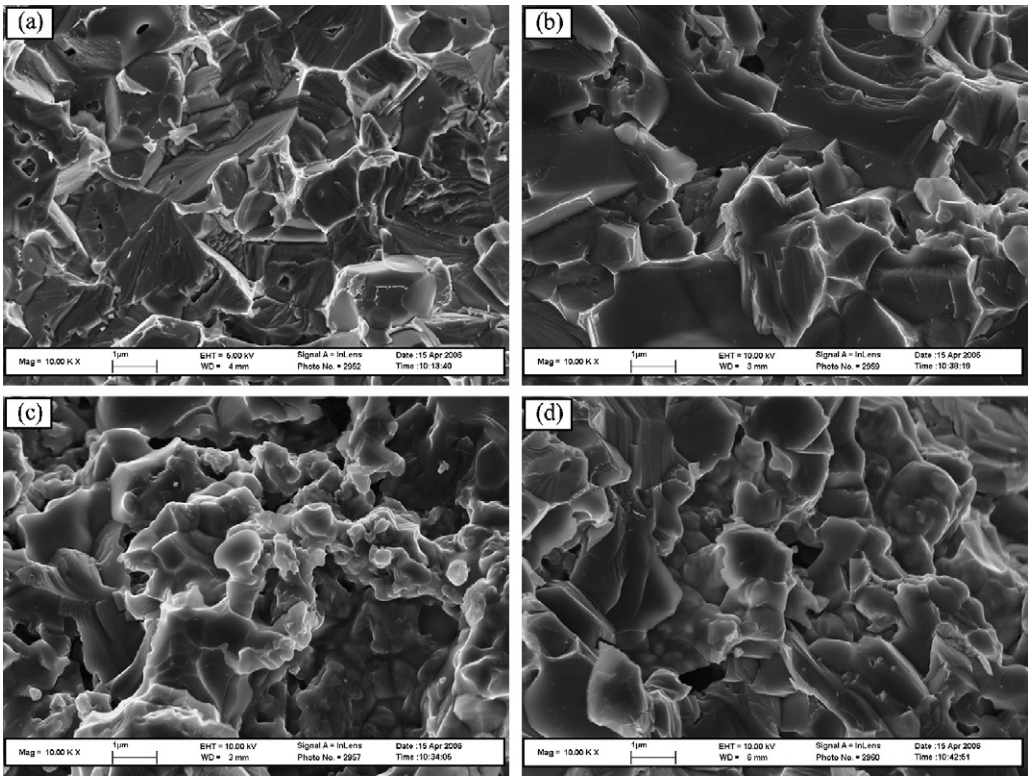

Fig. 3. SEM (SE) micrographs of fracture surfaces with various Zr content. (a) 0% Zr, (b) 10% Zr, (c) 15% Zr, (d) 20% Zr.

finer, and the amount of grains with core/rim structure decreases.

It is known that the black core is Ti(C, N) coming from the undissolved raw powders, the grey rim is the solid solution of carbonitride, which is formed during the liquid sintering process. The brighter color of white core obtained under SEM-BSE mode indicates that it contains much higher atomic number elements, and the binder is the mixture of Co and Ni [3,9,25].

The reason for the formation of white core/grey rim can be as follows: during the solid state sintering stage, W and Zr reacted with Ti(C, N) particles and then formed (Ti, W, Zr)(C, N) solid solutions which in turn served as precipitation sites. Then the rims are formed around the bright cores during the process of liquid sintering by dissolution–reprecipitation mechanism.

With regard to the coreless ceramic grains (Fig. 2b–d), the diffusion distance between W, Zr elements and some relatively small particles of Ti(C, N) is not long, as a result, the latter are completely consumed to form the coreless ceramic grains [9,25]. The decrease of grains with black core/grey rim structure indicates the reduction of the undissolved Ti(C, N) particles, which is basically influenced by Zr addition. Since Zr promotes the formation of (Ti, Zr, W)(C, N) and (Zr, Ti, W)(C, N) solid solutions, i.e. grey and bright coreless grains [26]. The amount of Zr-rich (Zr, Ti, W)(C, N) particles increases naturally as the level of added Zr increases. This provides more sites for the precipitation in the system. Consequently, the coreless grains are formed and the microstructure becomes finer.

3.3. Effect of Zr on the fracture surfaces of cermets

Fig. 3 shows the fracture surfaces of cermets. It is obviously observed that the fracture surface of cermets A and B is mainly transgranular fracture (Fig. 3a and b). However, the fracture surfaces show a finer morphology with increasing the addition of Zr and both intergranular and transgranular fractures are found (Fig. 3c and d). This is due to the refining effect of grains in cermets of Zr. Furthermore, some small pores exist in cermets B, C and D. The pores may be caused by the decrease of the wettability of binder (Co + Ni) on ceramic grains with increasing Zr content. Additionally, fine grains or sub-grains (about 100–300 nm) are observed from the fracture surface of cermets with high content of Zr element (Fig. 3c and d).

EDS results of cermet D analysis show that these fine grains or sub-grains are Zr-rich (Zr, Ti, W)(C, N) solid solutions in which Zr accounts for 64.2 wt% while Ti just accounts for 9.4 wt%. However, the larger grains which can be called (Ti, Zr, W)(C, N) solid solutions contains 61.2 wt% Ti and only 5.2 wt% Zr, as shown in Fig. 4. According to references [27,28], (Ti, Mo)(C, N) boundary phase, Ti(C, N)–WC–Co cermets and (Ti, Zr)N ternary system undergo a spinodal decomposition. Furthermore, Li and Huang [29] prepared the solid solution of (Ti, Zr)(C, N) which showed typical structure of spinodal decomposition. The sizes of raw powders in this study are all more than 2.46 μm and the size of Zr is even 7.40 μm. Additionally, it was denoted from Fig. 2c and d that most of the grains were larger than 1 μm. However, the grain size of these fine grains or sub-grains in Fig. 3c and d is only 100–300 nm. So we expect the spinodal decomposition

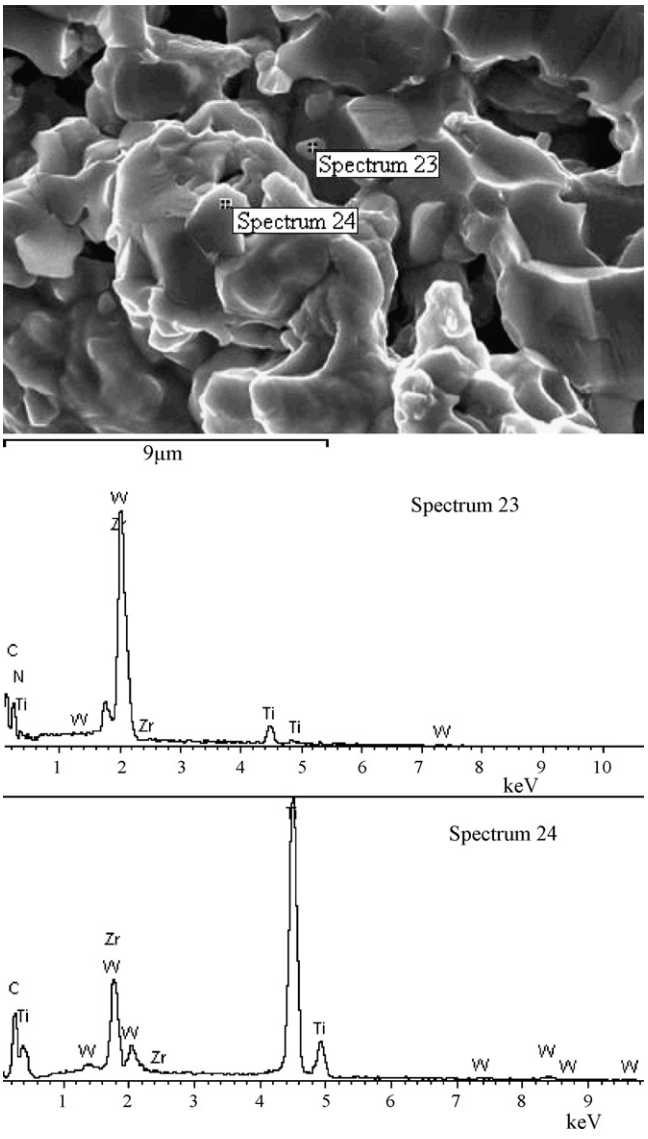

Fig. 4. EDS analysis of cermet D (20% Zr).

structure to occur in some large grains with high content of Zr element. It is known that the structure of the spinodal decomposition is based on uphill diffusion and its structure is the same as the mother phase. Usually, the size of the grains deriving from spinodal decomposition is in the range of a few nm. When the crack reaches the large grain with the structure of the spinodal decomposition, it will propagate along the interface of the spinodal decomposition area due to the internal stress in sub-micro grains. So the fracture shows a zigzag morphology and the micro fracture size is only 100–300 nm as shown in Fig. 3c and d.

Fig. 5 shows the crack propagation path of cermet C (15 wt% Zr) made by indentation, from which crack branching and crack deflection are observed clearly. Crack branching and crack deflection, which are usually caused by several factors such as local stress state, microstructure discontinuities (second phases, grain boundaries, inclusions, etc.) or environment [30], contribute a lot to the fracture toughness of cermets.

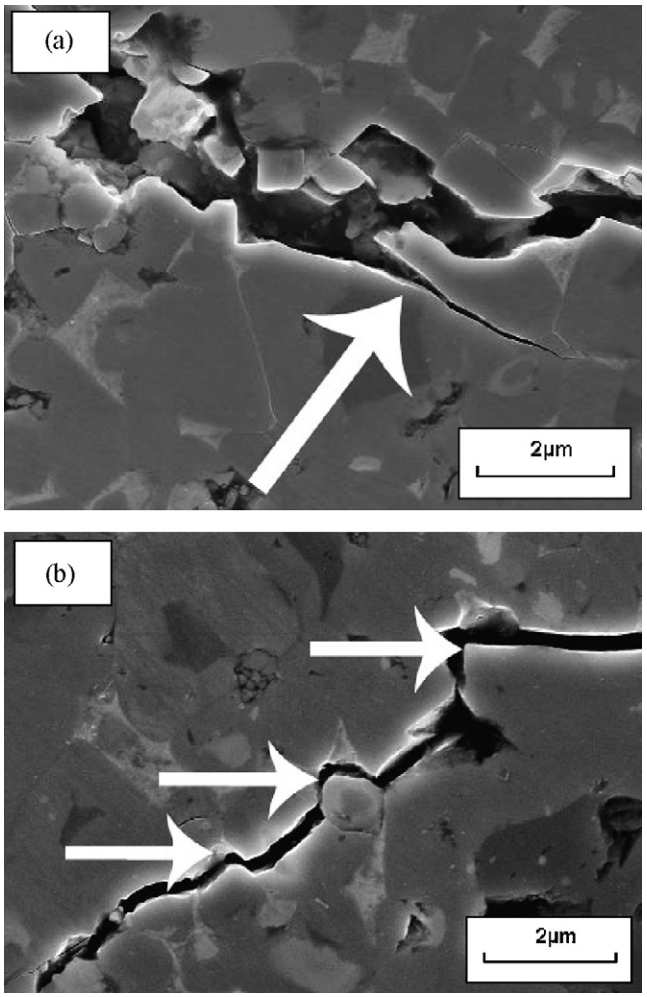

Fig. 5. Crack propagation path of cermet C (15% Zr). (a) Crack branching, (b) crack deflection.

3.4. Effect of Zr on the mechanical properties of cermets

Fig. 6 shows relative density and hardness of cermets. They present the same tendency with increasing Zr content. In general, the effects of Zr on the relative density and hardness are slight.

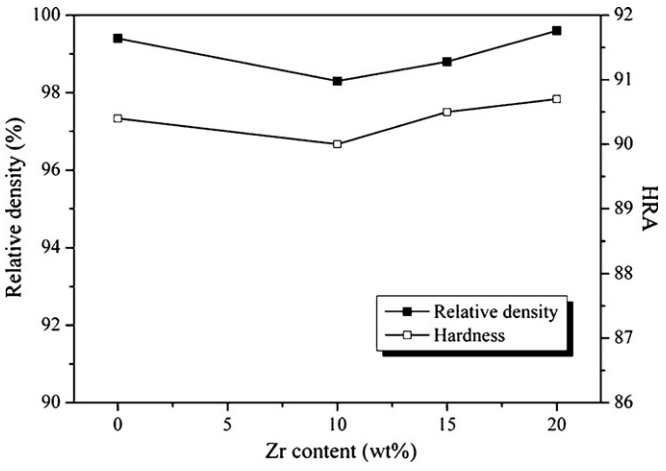

Fig. 6. Relative density and hardness of cermets.

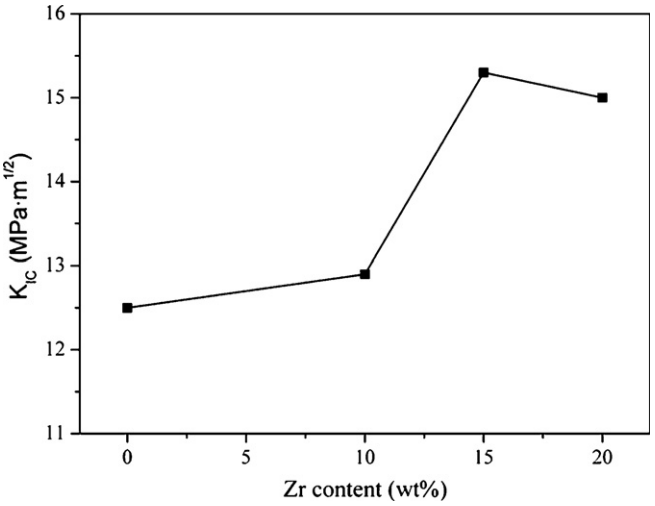

Fig. 7. Fracture toughness of cermets.

Fracture toughness is improved clearly when the amount of Zr reaches 15% and 20%, respectively, as shown in Fig. 7. The toughening mechanisms can be explained as follows: on the one hand, the presence of the coreless grains can be regarded as beneficial for the toughness of the cermets. The bonding force of the interface between core and rim is not as strong as that of the homogeneous grain, so it is easy to facilitate more crack initiation at the interface. It suggests that cermets consisting of one phase without the core/rim interface result in excellent fracture toughness [16]. On the other hand, crack branching and crack deflection can play an important role, too [17,30]. Since crack branching and crack deflection result in a somewhat rough fracture surface and lead to a higher fracture energy. Therefore, the zigzag of fracture caused by spinodal decomposition may play an active role in improving fracture toughness.

4. Conclusions

The microstructure of cermets with Zr addition consists of complex microstructure, i.e. black core/grey rim ceramic, white core/grey rim ceramic, grey coreless ceramic, bright coreless ceramic and white binder. The amount of grains with core/rim structure decreases while that of coreless grains increases with Zr content increase. The microstructure becomes finer with increasing Zr content and the size of some fine grains is just about 100 nm, this is supposed to be associated with a spinodal decomposition in cermets.

The relative density and hardness is not influenced by increasing Zr content but the fracture toughness is clearly improved. The increase of the coreless grains, the spinodal decomposition in Zr-rich ceramic grains, as well as the crack deflection and crack branching mechanisms are responsible for the improved fracture toughness.

Acknowledgments

Support for this work by Nippon Sheet Glass Foundation (NSGF), Natural Science Foundation of China under contracts nos. 301–00287 and 50072003, respectively, are gratefully acknowledged.

References

[1] P. Ettmayer, H. Kolaska, W. Lengauer, K. Dreyer, Ti(C, N) cermets—metallurgy and properties, Int. J. Refract. Met. Hard Mater. 13 (1995) 343–351.
[2] P. Lindahl, P. Gustafson, U. Rolander, L. Stals, H.-O. Andrén, Microstructure of model cermets with high Mo or W content, Int. J. Refract. Met. Hard Mater. 17 (1999) 411–421.
[3] N. Liu, Y.D. Xu, Z.H. Li, M.H. Chen, G.H. Li, L.D. Zhang, Influence of molybdenum addition on the microstructure and mechanical properties of TiC-based cermets with nano-TiN modification, Ceram. Int. 29 (2003) 919–925.
[4] S.Y. Ahn, S. Kang, Effect of WC particle size on microstructure and rim composition in the Ti($C_{0.7}N_{0.3}$)–WC–Ni system, Scripta Mater. 55 (2006) 1015–1018.
[5] Y. Zheng, W.H. Xiong, W.J. Liu, W. Lei, Q. Yuan, Effect of nano addition on the microstructures and mechanical properties of Ti(C, N)-based cermets, Ceram. Int. 31 (2005) 165–170.
[6] J. Xiong, Z.X. Guo, B.L. Shen, D. Cao, The effect of WC, Mo_2C, TaC content on the microstructure and properties of ultra-fine $TiC_{0.7}C_{0.3}$ cermet, Mater. Des. 28 (2007) 1689–1694.
[7] D. Mari, S. Bolognini, G. Feusier, T. Cutard, T. Viatte, W. Benoit, TiMoCN based cermets. Part II. Microstructure and room temperature mechanical properties, Int. J. Refract. Met. Hard Mater. 21 (2003) 47–53.
[8] J.H. Gong, X.T. Pan, H.Z. Miao, Z. Zhao, Effect of metallic binder content on the microstructure of TiCN-based cermets, Mater. Sci. Eng. A 359 (2003) 391–395.
[9] N. Liu, W.H. Yin, L.W. Zhu, Effect of TiC/TiN powder size on microstructure and properties of Ti(C,N)-based cermets, Mater. Sci. Eng. A 445–446 (2007) 707–716.
[10] N. Liu, Q.M. Zeng, X.M. Huang, Microstructure in carbonitride cermets, Mater. Sci. Tech. 17 (9) (2001) 1050–1054.
[11] N. Liu, K. Cui, Z.H. Hu, Effect of Er on strengthening of interface of Ti(C, N) based cermets, Trans. Nonferr. Met. Soc. China 6 (3) (1996) 72–76.
[12] K. Jia, T.E. Fischer, B. Gallois, Microstructure, hardness and toughness of nanostructured and conventional WC–Co composites, Nanostruct. Mater. 10 (1998) 875–879.
[13] D. Mari, S. Bolognini, T. Viatte, W. Benoit, Study of the mechanical properties of TiCN–WC–Co hard metals by the interpretation of internal friction spectra, Int. J. Refract. Met. Hard Mater. 19 (4–6) (2001) 257–265.
[14] D. Mari, S. Bolognini, G. Feusier, T. Cutard, C. Verdon, T. Viatte, W. Benoit, TiMoCN based cermets. Part I. Morphology and phase composition, Int. J. Refract. Met. Hard Mater. 21 (2003) 37–46.
[15] Y.K. Kim, J.H. Shim, Y.W. Cho, H.S. Yang, J.K. Park, Mechanochemical synthesis of nanocomposite powder for ultrafine (Ti, Mo)C–Ni cermet without core–rim structure, Int. J. Refract. Met. Hard Mater. 22 (2004) 193–196.
[16] S. Park, S. Kang, Toughened ultra-fine (Ti, W)(CN)–Ni cermets, Scripta Mater. 52 (2005) 129–133.
[17] D.J. Green, An Introduction to the Mechanical Properties of Ceramics, Cambridge University Press, Cambridge, 1998.
[18] J.H. Gong, Fracture Mechanics of Ceramics, Tsinghua University Press, Beijing, 2001.
[19] W. Chaisan, R. Yimnirun, S. Ananta, D.P. Cann, The effects of the spinodal microstructure on the electrical properties of TiO_2–SnO_2 ceramics, J. Solid State Chem. 178 (2005) 613–620.
[20] A.M. Mebed, T. Koyama, T. Miyazaki, Spinodal decomposition existence of the βTi–Cr binary alloy: computer simulation of the real alloy system and experimental investigations, Comput. Mater. Sci. 14 (1999) 318–322.
[21] T. Ujihara, K. Osamura, Assessing composition gradient energy effects due to spin interaction on the spinodal decomposition of Fe–Cr, Mater. Sci. Eng. A 312 (2001) 128–135.

[22] J.C. Zhao, M.R. Notis, Spinodal decomposition, ordering transformation, and discontinuous precipitation in a Cu–15Ni–8Sn alloy, Acta Mater. 46 (1998) 4203–4218.
[23] E. Rudy, Boundary phase stability and critical phenomena in high-order solid solution systems, J. Less-Common Met. 33 (1973) 43.
[24] D.K. Shetty, I.G. Wright, P.N. Mincer, A.H. Clauer, Indentation fracture of WC–Co cermets, J. Mater. Sci. 20 (1985) 1873–1882.
[25] S. Chao, N. Liu, Y.P. Yuan, C.L. Han, Y.D. Xu, M. Shi, J.P. Feng, Microstructure and mechanical properties of ultra-fine Ti(CN)-based cermets fabricated from nano/submicron starting powders, Ceram. Int. 31 (2005) 851–862.
[26] F. Qi, S. Kang, A study on microstructural changes in Ti(CN)–NbC–Ni cermets, Mater. Sci. Eng. A 251 (1998) 276–285.
[27] P. Wally, P. Ettmayer, W. Lengauer, The Ti–Mo–C–N system: stability of the (Ti, Mo)(C, N)$_{1-x}$ phase, J. Alloys Comp. 228 (1995) 96–101.
[28] G.Y. Yang, E. Etchssahar, A miscibility gap in the FCC nitride region of the ternary system titanium–zirconium–nitrogen, Scripta Metall. 31 (7) (1994) 903–908.
[29] J.B. Li, Y. Huang, Research and development of intelligent/smart materials, Chin. J. Mater. Res. 9 (Suppl.) (1995) 233–240.
[30] A. Celli, A. Tucci, L. Esposito, C. Palmonari, Fracture analysis of cracks in alumina–zirconia composites, J. Euro. Ceram. Soc. 23 (2003) 469–479.